Supplemental Material for "Prediction of the material with highest known melting point from ab initio molecular dynamics calculations"

Qi-Jun Hong and Axel van de Walle

June 20, 2015

1 Methods

1.1 The Small-size Coexistence Method

We employ the small-size coexistence method to calculate the melting temperatures [1]. Based on this method, we have developed and distributed online an automated computer code called SLUSCHI (Solid and Liquid in Ultra Small Coexistence with Hovering Interfaces). While the traditional two-phase coexistence method accurately predicts melting temperature based on stabilized coexistence, it is computationally prohibitive in the DFT framework, due to the large system size (usually at least 1,000 atoms) required to stabilize the interface. We reduce the cell size down to about 100 atoms, so it becomes accessible directly with DFT. Although coexistence can no longer be stabilized in a small cell, we formally recover the melting temperature based on the probability that the system completely melts or solidifies as a function of temperature. We run multiple duplicates of small-cell coexistences to evaluate the probabilities of the final phases. Starting from solid-liquid coexistence, we monitor the system evolution until it reaches a pure final phase, either solid or liquid, and we calculate such probabilities based on the results from multiple duplicated simulations. We then fit these probability distributions to a known theoretically-derived functional form that yields the melting point. The reader may refer to Ref. [1] for detailed derivation, validation and examples. It should be noted that, for compositions where melting is not congruent, the small-size coexistence method provides the temperature at which the solid and liquid free energy are equal, which lies between the solidus and the liquidus. However, at extrema in the melting point (which is our target), the solidus and the liquidus coincide and the small-size coexistence method necessarily yields the melting point.

Details on the small-cell coexistence method and SLUSCHI can be found in Appendix 1.

1.2 Density Functional Theory Calculations

We employ first-principles DFT [2] to model electronic interactions. All electronic structures are calculated by the Vienna *Ab-initio* Simulation Package (VASP) [3, 4], with the projector-augmented-wave (PAW) [6] implementation and the generalized gradient approximation (GGA) for exchange-correlation energy, in the form known as PBE [5]. Only the valence electrons are relaxed for electronic structure optimization. The electronic temperature is accounted for by imposing a Fermi distribution of the electrons on the energy level density of states, so it is consistent with the ionic temperature. All melting point calculations are performed on supercells with 64 cations (Hf and Ta) and 64 anions (C, N and vacancies). The planewave energy cutoff is set to 400 eV during the MD simulations, and it is further increased to 500 eV to count for the Pulay stress [7].

1.3 Molecular Dynamics Simulations

First-principles MD techniques are utilized to simulate atomic movements and trajectories. Specifically, MD simulations are carried out under constant number of atoms, pressure and temperature condition (NPT, isothermal-isobaric ensemble). Here the thermostat is conducted under the Nose-Hoover chain formalism [8, 9, 10, 11]. The barostat is realized by adjusting volume every 200 steps according to average pressure. Although this does not formally generate an isobaric ensemble, this approach has been shown to provide an effective way to change volume smoothly and to avoid the unphysical large oscillation caused by commonly used barostats [1].

2 HSE correction on melting temperature

We evaluate the HSE functional's impact on melting temperature as

$$\frac{T_m^{HSE}}{T_m^{PBE}} = \frac{\Delta H^{HSE}}{\Delta H^{PBE}},$$

where ΔH is heat of fusion and T_m is melting temperature. Though it is prohibitive to compute ΔH^{HSE} directly, we calculate the energy correction on the solid and the liquid phases separately

$$H^{HSE} - H^{PBE} = \left\langle H^{HSE} - H^{PBE} \right\rangle_{H^{PBE}}.$$

The bracket $\langle \cdots \rangle_{H^{PBE}}$ means that we randomly choose snapshots from MD trajectories of PBE, and calculate the energy differences between the two functionals.

The calculated HSE corrections are listed in Table S1. An average correction of 460 K is found.

Table S1: HSE correction on melting temperature.

material	T_m / K	ΔH / eV	$\langle H^{HSE} - H^{PBE} \rangle_{H^{PBE}}$ / eV		T_m correction / K
			solid	liquid	
HfC	3842	0.798	-1.566	-1.482	401
$HfC_{0.94}$	3861	0.808	-1.558	-1.452	502
$HfC_{0.88}$	3898	0.811	-1.531	-1.438	448
$HfC_{0.81}$	3962	0.786	-1.510	-1.416	470
$HfC_{0.75}$	3921	0.720	-1.489	-1.399	492

3 Melting temperature calculations of Hf-C, Hf-Ta-C and Hf-C-N

We list in Table S2 our calculation results of the melting temperatures, which we use to generate Fig. 1, 4 and 5 in the main text. The details of the calculations are presented in the Appendix.

Table S2: Melting temperatures from small-cell coexistence calculations.

chemical formula	melting temperature / K
HfC	3842 ± 25
$HfC_{0.97}$	3850 ± 34
$HfC_{0.94}$	3861 ± 21
$HfC_{0.91}$	3876 ± 24
$HfC_{0.88}$	3898 ± 13
$HfC_{0.84}$	3950 ± 17
$HfC_{0.81}$	3962 ± 27
$HfC_{0.78}$	3936 ± 12
$HfC_{0.75}$	3921 ± 14
$Hf_{0.88}Ta_{0.12}C_{0.88}$	3910 ± 17
$Hf_{0.75}Ta_{0.25}C_{0.88}$	3920 ± 16
$Hf_{0.62}Ta_{0.38}C_{0.88}$	3900 ± 15
$Hf_{0.5}Ta_{0.5}C_{0.88}$	3859 ± 14
$Hf_{0.25}Ta_{0.75}C_{0.88}$	3893 ± 11
$Hf_{0.19}Ta_{0.81}C_{0.88}$	3895 ± 16
$TaC_{0.88}$	3830 ± 24
$HfC_{0.75}N_{0.22}$	4039 ± 26
$HfC_{0.62}N_{0.19}$	4081 ± 12
$HfC_{0.56}N_{0.38}$	4141 ± 21
$HfC_{0.56}N_{0.25}$	4082 ± 28
$HfC_{0.5}N_{0.25}$	4055 ± 24
$HfC_{0.44}N_{0.5}$	4106 ± 14
$HfC_{0.44}N_{0.19}$	3847 ± 26
$HfC_{0.38}N_{0.38}$	4008 ± 19
$Hf_{0.75}Ta_{0.25}C_{0.56}N_{0.25}$	3980 ± 13

4 Quadratic fitting of melting temperature in the Hf-C-N system

The quadratic function in main text Fig. 5 is fitted to the following expression.

$$T_m = k_1(x\cos\theta + y\sin\theta - a_1)^2 + k_2(-x\sin\theta + y\cos\theta - a_2)^2 + T_0,$$

where x and y are compositions in HfC_xN_y. The values of the fitting parameters are

$$T_0 = 4135, k_1 = -947, k_2 = -7302, a_1 = 0.654, a_2 = 0.0456, \theta = -0.285\pi.$$

A 2-D version of the melting temperature surface (in K) is shown in Fig. S1.

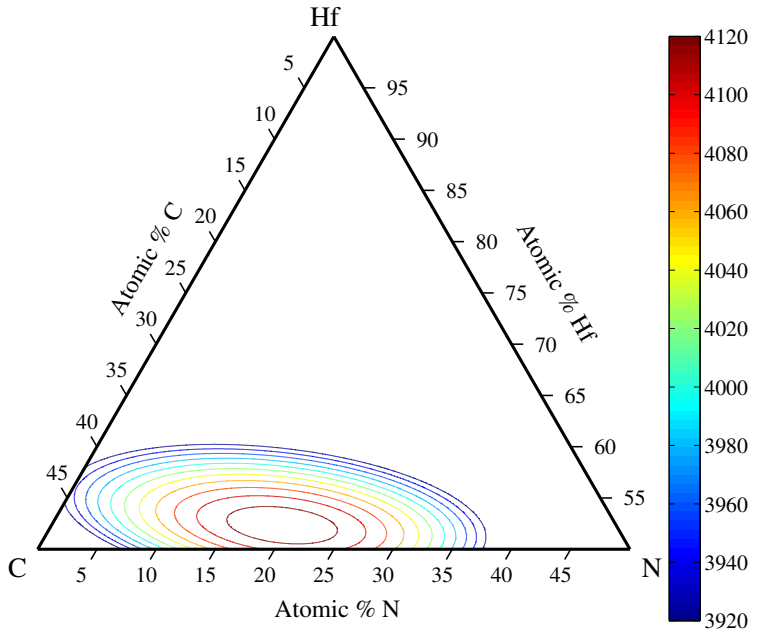

Figure S1: 2-D version of the fitted melting temperature surface.

5 Comparison between the Hf-C and Hf-C-N systems: heat of fusion and liquid-state entropy

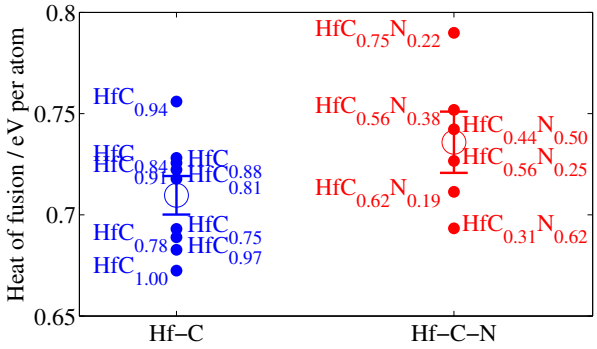

Figure S2: Heat of fusion in Hf-C (blue) and Hf-C-N (red) systems. Each solid dot corresponds to one compound, while an open circle with error bar is the average and standard error. The addition of nitrogen increases the heat of fusion by 4%, which is comparable to the increment of melting temperature.

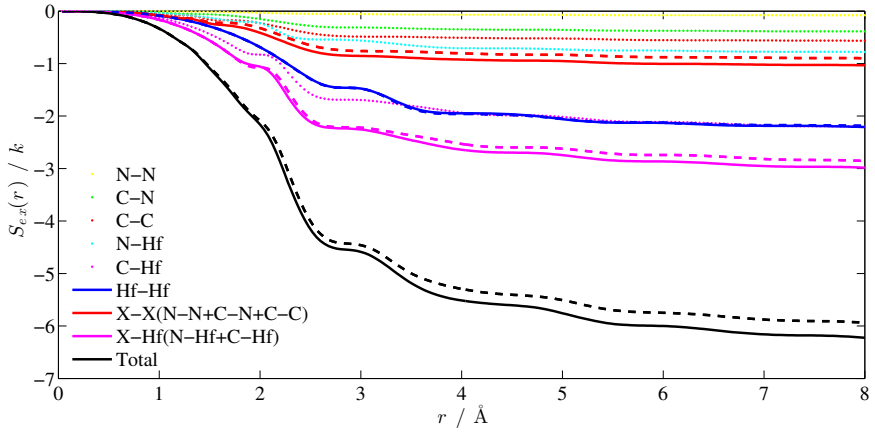

Figure S3: Comparison of the entropies of liquid-state $Hf_{32}C_{31}$ (dash lines) and $Hf_{32}C_{24}N_7$ (dot and solid lines). Shown are excess entropies (with respect to ideal gas) calculated from pair-correlation functions, according to the relation $S_{ex}/k_B = -2\pi\rho \sum_{i,j} x_i x_j \int_0^\infty \Big(g_{ij}(r) \ln g_{ij}(r) - \big[g_{ij}(r) - 1 \big] \Big) r^2 \, \mathrm{d}r$, where ρ is density, x_i is fractional composition, and g_{ij} is pair correlation function between species i and j. It is evident that nitrogen brings down the total entropy (black), through anion-anion (X−X, red) and anion-cation (X−Hf, purple) pairs, while leaving the cation-cation (Hf−Hf, blue) contribution nearly untouched.

References

[1] Q.-J. Hong, and A. van de Walle, Solid-liquid coexistence in small systems: A statistical method to calculate melting temperatures. J. Chem. Phys. **139**, 094114 (2013).

[2] W. Kohn, and L. J. Sham, Self-consistent equations including exchange and correlation effects. Phys. Rev. **140**, A1133-A1138 (1965).

[3] G. Kresse, and J. Furthmüller, Efficient iterative schemes for ab initio total-energy calculations using a plane-wave basis set. Phys. Rev. B **54**, 11169-11186 (1996).

[4] G. Kresse, and D. Joubert, From ultrasoft pseudopotentials to the projector augmented-wave method. Phys. Rev. B **59**, 1758-1775 (1999).

[5] J. P. Perdew, K. Burke, and M. Ernzerhof, Generalized gradient approximation made simple. Phys. Rev. Lett. **77**, 3865-3868 (1996).

[6] P. Blöchl, Projector augmented-wave method. Phys. Rev. B **50**, 17953-17979 (1994).

[7] G. P. Francis, and M. C. Payne, Finite basis set corrections to total energy pseudopotential calculations. J. Phys.: Condens. Matter **2**, 4395-4404 (1990).

[8] S. Nosé, A molecular-dynamics method for simulations in the canonical ensemble. Mol. Phys. **52**, 255-268 (1984).

[9] S. Nosé, A unified formulation of the constant temperature molecular-dynamics methods. J. Chem. Phys. **81**, 511-519 (1984).

[10] W. G. Hoover, Canonical dynamics - equilibrium phase-space distributions. Phys. Rev. A **31**, 1695-1697 (1985).

[11] G. J. Martyna, M. L. Klein, and M. Tuckerman, Nose-Hoover chains - the canonical ensemble via continuous dynamics. J. Chem. Phys. **97**, 2635-2643 (1992).

Appendix 1

SLUSCHI (Solid and Liquid in Ultra Small Coexistence with Hovering Interfaces) is a fully automated code which calculates melting points based on first-principles molecular dynamics simulations, with interface to the first-principles code VASP. Starting from the crystal structure of a solid (which the user inputs), SLUSCHI will automatically build a supercell of a proper size, prepare solid-liquid coexistence, and then employ the small-cell coexistence method (Q.-J. Hong and A. van de Walle, *J. Chem. Phys.* **139**, 094114 (2013)) to calculate the melting temperature.

SLUSCHI is applicable to a wide variety of materials, thanks to the fact that density functional theory calculations are highly generalizable. The MD simulations account for all types of defects and sources of entropy, and the calculations take all effects (and their delicate balance) into account. This is precisely why accurate large-scale molecular dynamics is employed.

SLUSCHI has been studied and tested on more than ten systems and several dozen materials, including
• Al • Si • Ti (bcc) • Ta (various pseudopotentials, under ambient pressure and 200 GPa, bcc)
• Na (30-120 GPa, bcc/fcc) • NaCl • $La_2Zr_2O_7$ (La_2O_3-$2ZrO_2$, pyrochlore structure)
• Ru and its ternary alloys,
in addition to the Hf-Ta-C-N systems. Here we list in Table S3 the computational results, with comparison to experiments. Details (DFT setup, pseudopotentials, computer cost, etc.) can be found at the SLUSCHI webpage (http://blogs.brown.edu/qhong/). It is convincing that SLUSCHI can generally achieve an accuracy of around 100 K in melting point calculations.

Table S3: Melting temperatures based on SLUSCHI calculations and comparison to experiments.

systems	SLUSCHI / K	after HSE correction / K	experiment / K
Al	999 ± 21	1054	933
Ti_v[a]	1750 ± 25	1971	1941
Ti_pv[b]	1932 ± 38		1941
Si	1378 ± 24	1785	1687
Ru_v[a]	2435 ± 32		2607
Ru_pv[b]	2550 ± 34		2607
Ta_v[a]	2986 ± 41		3290
Ta_pv[b]	3194 ± 40		3290
Na (15 GPa)	657 ± 8		810, 698[c]
NaCl	1014 ± 18		1074
$La_2Zr_2O_7$	2420 ± 27	2630	2530

[a] Pseudopotentials with valence electrons relaxed.
[b] Pseudopotentials with inner core p electrons relaxed in addition.
[c] Melting temperature value under dispute due to high reactivity of the material and the extreme condition.

Appendix 2

Here we present the details of our melting point calculations. Each figure has a one-to-one correspondence to the materials listed in Table S2.

The Hf-C system

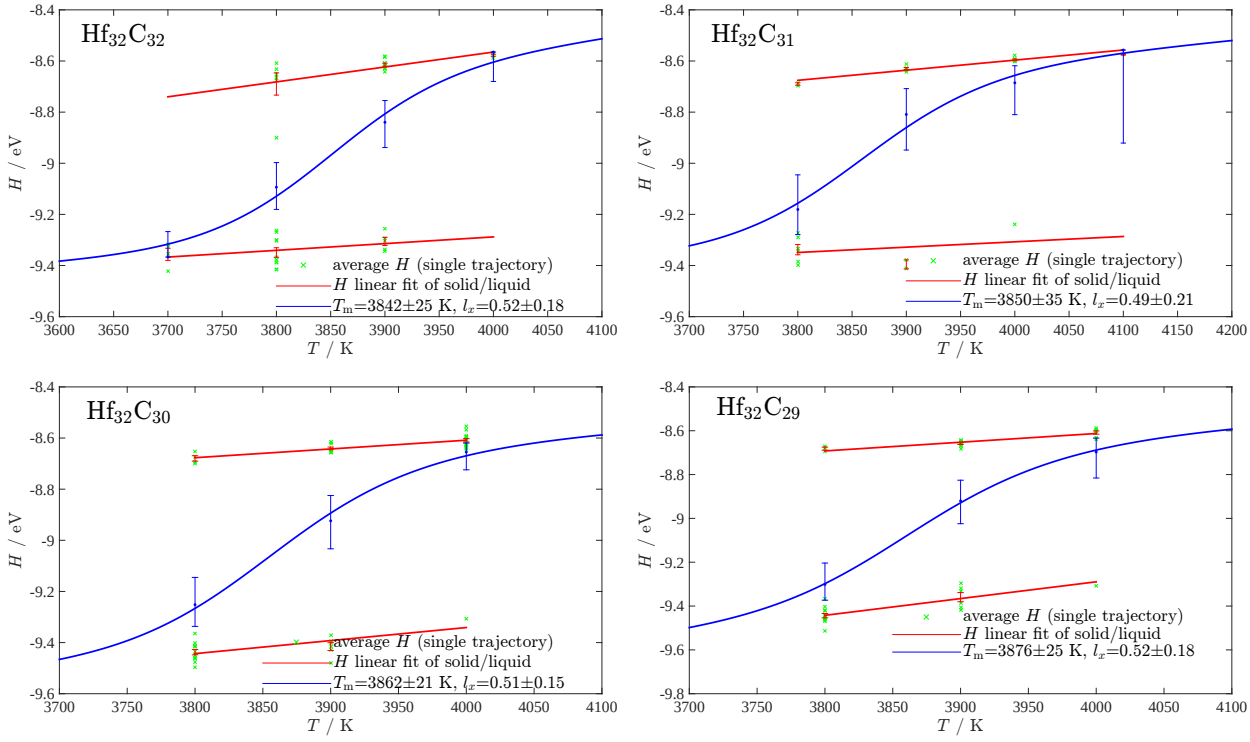

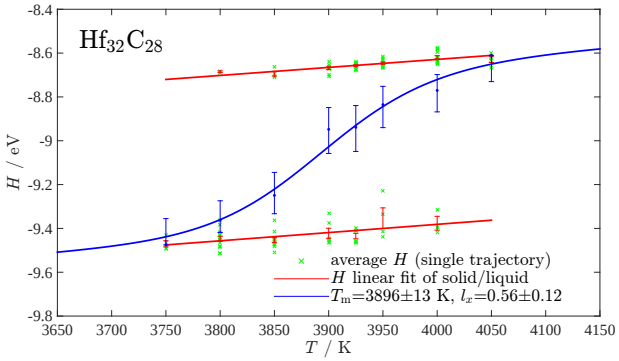
Hf32C28
H / eV
T / K
average H (single trajectory)
H linear fit of solid/liquid
Tm=3896±13 K, lx=0.56±0.12

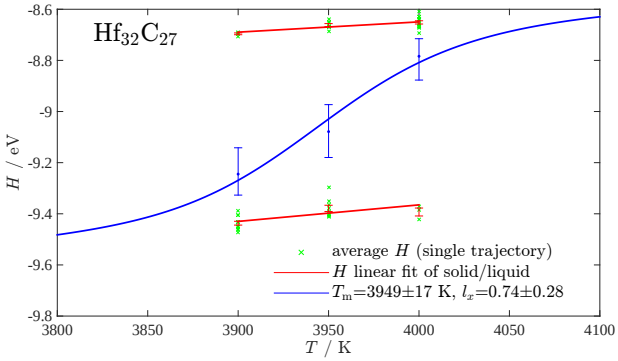
Hf32C27
H / eV
T / K
average H (single trajectory)
H linear fit of solid/liquid
Tm=3949±17 K, lx=0.74±0.28

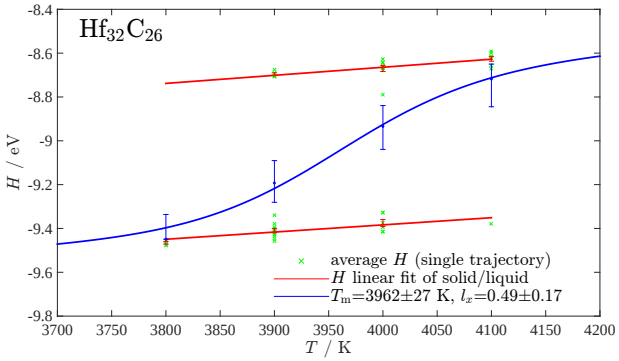
Hf32C26
H / eV
T / K
average H (single trajectory)
H linear fit of solid/liquid
Tm=3962±27 K, lx=0.49±0.17

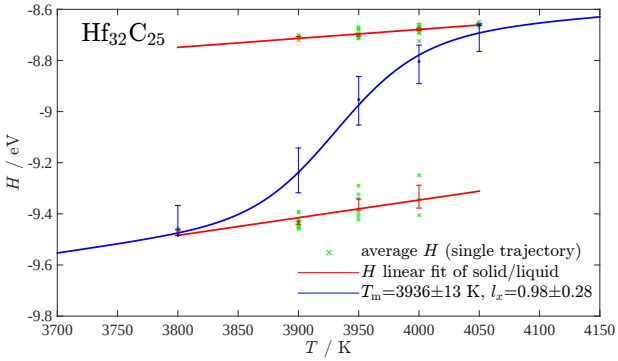
Hf32C25
H / eV
T / K
average H (single trajectory)
H linear fit of solid/liquid
Tm=3936±13 K, lx=0.98±0.28

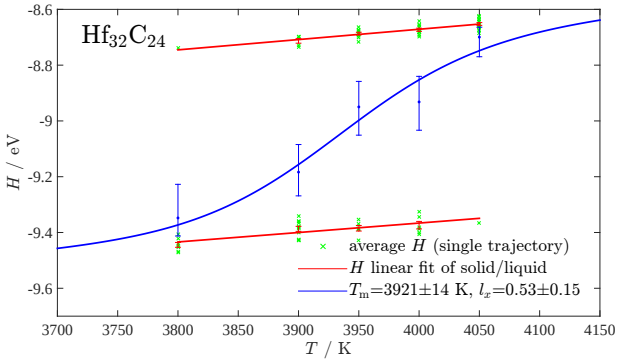
Hf32C24
H / eV
T / K
average H (single trajectory)
H linear fit of solid/liquid
Tm=3921±14 K, lx=0.53±0.15

The Hf-Ta-C system

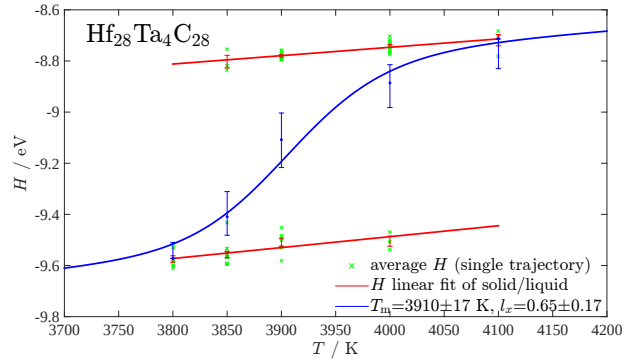

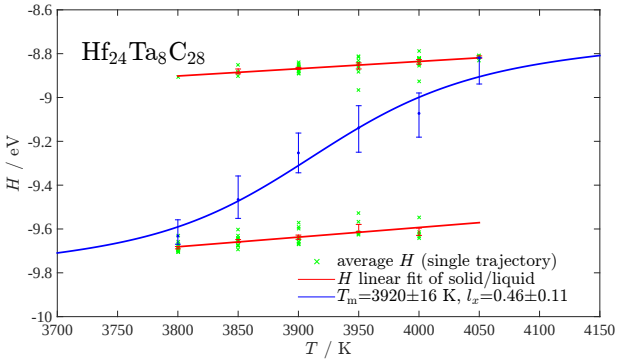

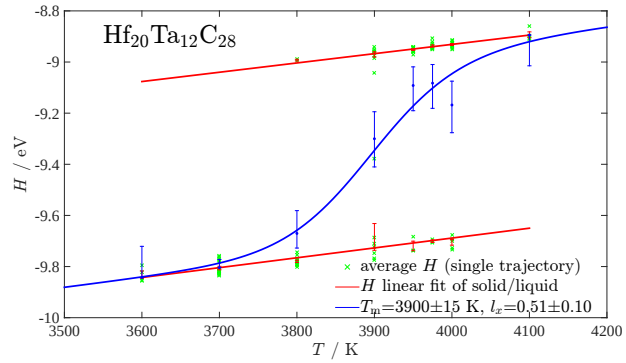

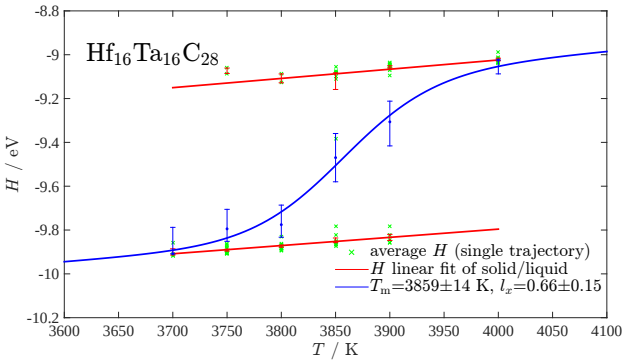

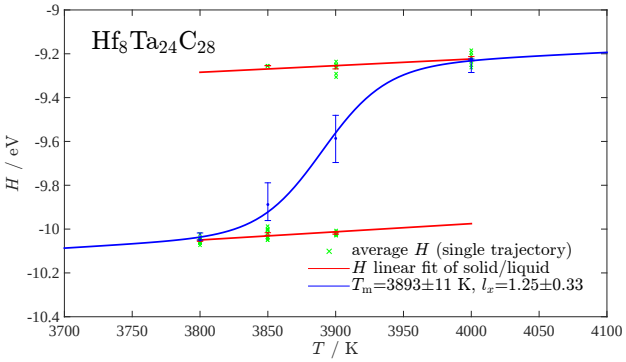

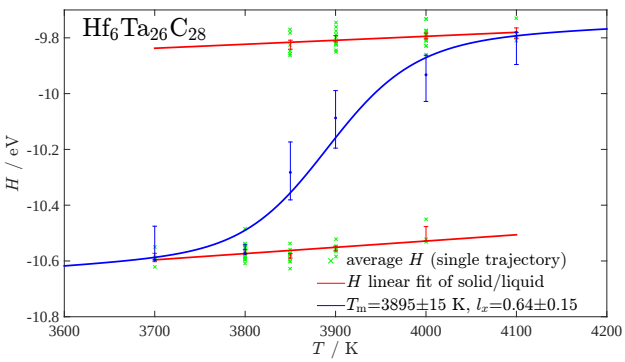

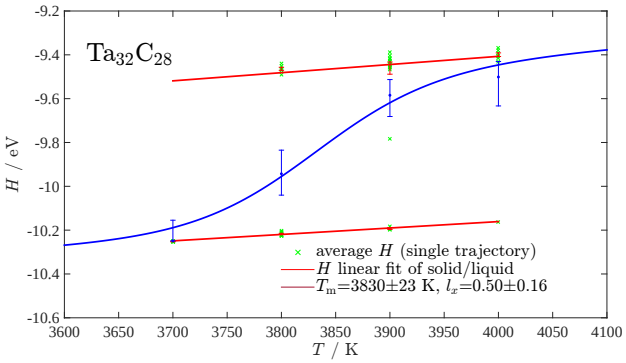

The Hf-C-N system

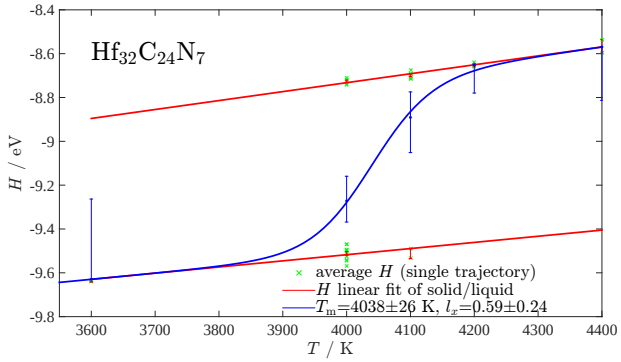

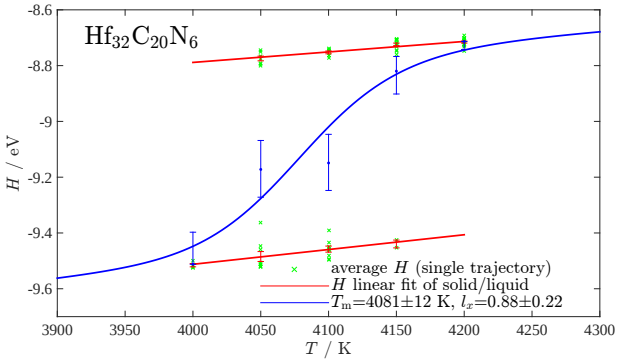

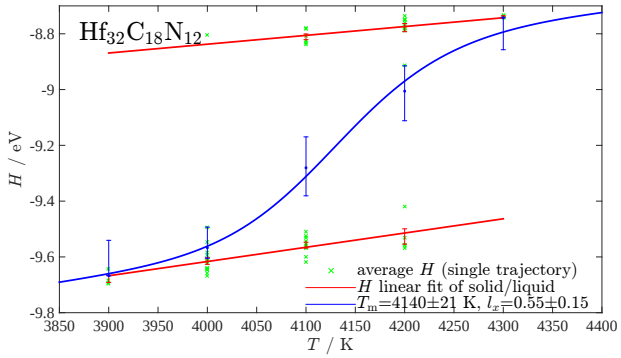

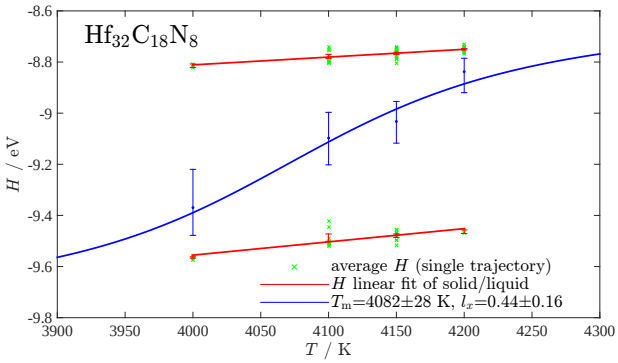

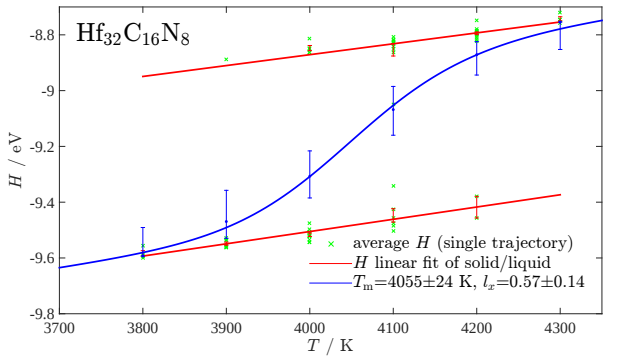

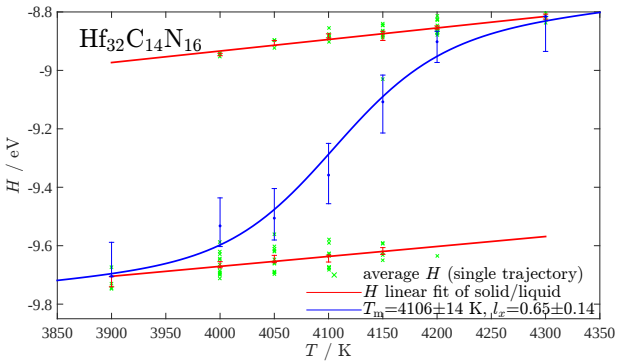

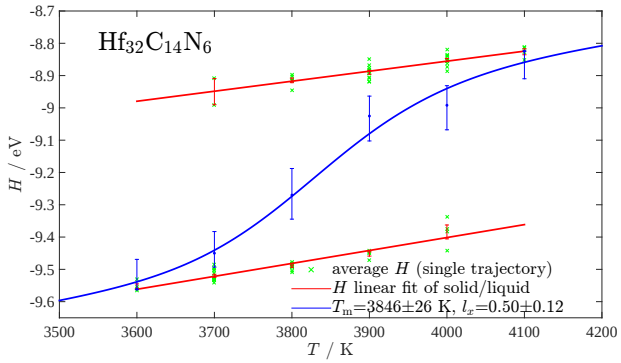

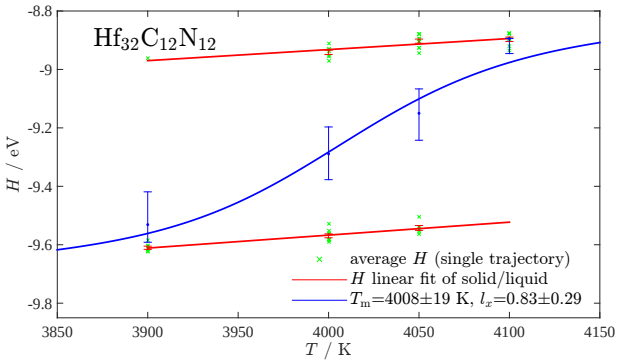

The Hf-Ta-C-N system